STAT3 regulates miR93-mediated apoptosis through inhibiting DAPK1 in renal cell carcinoma

Yang Du
First Hospital of China Medical University
Chuize Kong (kongchuize_cmu@sina.cn)
First Affiliated Hospital of China Medical University https://orcid.org/0000-0002-0875-2173

Research

Keywords: MicroRNA, renal cell carcinoma, DAPK1, STAT3, apoptosis

Posted Date: April 16th, 2020

DOI: https://doi.org/10.21203/rs.3.rs-22966/v1

Version of Record: A version of this preprint was published at Cancer Gene Therapy on November 23rd, 2020. See the published version at https://doi.org/10.1038/s41417-020-00235-y.

STAT3 regulates miR93-mediated apoptosis through inhibiting DAPK1 in renal cell carcinoma

Yang Du[1], Chuize Kong[1]

1.Department of Urology, First Hospital of China Medical University, Shenyang, 110001, China

Corresponding author： Professor Chuize Kong

Department of Urology, First Hospital of China Medical University, Shenyang, 110001, China

kongchuize_cmu@sina.cn

ABSTRACT

Signal transducer and activator of transcription 3, STAT3, is an essential member of the STAT family. STAT3 regulates diverse genes mediating inflammatory reaction, cell survival, proliferation, and angiogenesis, and it is aberrantly upregulated and activated in various types of malignancies. Meanwhile, STAT3 signaling is involved in multiple feedback loops and pathways. In this study, we demonstrate that in renal cell carcinoma, miR-93-3p act an oncogenesis role in renal cell carcinoma. It enhanced RCC cell proliferation and suppressed apoptosis. Besides, STAT3 could regulate the transcription of miR-93 by directly binding with its promoter region.

miR-93 can inhibit the protein level of death-associated protein kinase 1, DAPK1. What's more, STAT3 could block the expression of DAPK1 on the level of RNA. Importantly, we verify that, through over-expression, DAPK1 might, in return, suppress the activated-STAT3 entering cell nucleus. Thus, the study uncovers a potential signaling transduction pathway, STAT3-miR93-DAPK1, which is continuously activated, and may provide a novel clinical therapeutic approach for RCC.

Keywords

MicroRNA, renal cell carcinoma, DAPK1, STAT3, apoptosis

Introduction

Renal cell carcinoma (RCC) accounts for 2–3% of all adult malignancies, and the incidence of RCC ranks third of the urinary tumor, only following prostate and bladder carcinoma in China. Statistics data from the Chinese National Cancer spectrum show that the incidence of RCC has increased by 6.5% per year over the past 20 years and with 40% of patients dying from RCC. Early diagnosis became the best chance for curing. However, patients with early-stage RCC lack typical clinical symptoms, such as pain, the presence of a mass, or haematuria. Unfortunately, more than 30% of RCC patients have metastatic lesions once diagnosed. Therefore, the development of efficient clinical diagnostic strategies is critical for the prevention and management of RCC [1-3].

MicroRNAs (miRNAs) are a class of highly conserved endogenous small non-coding RNAs, existing in almost all organisms. They function as negative regulators of gene expression by base pairing and binding with the 3′-untranslated region (3′-UTR) of target mRNA, causing RNA degradation or translation suppression. Accumulating

evidence has demonstrated that miRNAs play essential roles in biological processes, such as differentiate, proliferation, and apoptosis. The dysregulation of miRNAs is recognized as the crucial factor in the development and progression of diverse cancers [4-8]. The miR-106a-25 cluster encodes for three miRNAs, miR-106b, miR-93, and miR-25, and is embedded within the 13th intron of Mini-chromosome Maintenance protein 7 (MCM7) gene [9, 10]. MiR-93 is up-regulated in many human cancers, such as gastric, breast, prostate, and ovarian tumors [11-14]. It acts as an oncogene to modulate cell apoptosis, cell cycle, and proliferation. However, the function of miR-93-3p in RCC and its associated with signalling pathway remain unknown.

Methods

Cell Lines

The human renal carcinoma cell lines (786-O, ACHN, 769-P, OSRC-2, and CAKI-1) and the proximal tubule epithelial cell line (HK-2) were obtained from the Chinese Academy of Sciences Committee on Type Culture Collection cell bank (Shanghai, China). All media were supplemented with 100 U/ml penicillin, and 100 mg/ml streptomycin (TBDscience, Tianjin, China), and cells were cultured at 37°C in 5% CO_2.

Tissue samples and clinical data collection

In this study, we analyzed 96 patients who underwent surgical resection and were diagnosed pathologically with RCC at the First Hospital of Chinese Medical University from 2016 to 2017, and collected tissue samples were stored at -80°C until used. The study was approved and supervised by the Ethics Committee on Human Research of the First Affiliated Hospital of Chinese Medical University, and 96 patients volunteered for this study and had written informed consent.

RNA preparation and quantitative real-time polymerase chain reaction

mRNA was obtained from clinical samples and treated cells with RNAiso Plus (Takara, Dalian, Liaoning, China). cDNA was synthesized with PrimeScript™ RT Master Mix (Takara, Dalian, Liaoning, China), and quantitative real-time PCR was performed using SYBR Premix EX Taq™ (Takara, Dalian, Liaoning, China). microRNA was extracted using a miRNeasy™ Mini Kit (Qiagen, Hilden, Germany). cDNA synthesis and quantitative real-time PCR were performed using Mir-X™ miRNA First-Strand Synthesis Kit and SYBR® Premix Ex Taq™ II (Takara, Dalian, Liaoning, China) according to the manufacturer's protocol. All data were normalized to the expression of beta-actin(**β**-actin) and U6. The relative expression was evaluated using the $2^{-\Delta\Delta Ct}$ method. The primers for target genes and the internal reference used in this study were as follows: DAPK1 F: 5'-AGAAATTCAAGAAGTTTGCAG-3'; R: 5'-GTCTTCCTCATCCAGAGTAT-3', STAT3 F: 5'-ATCACGCCTTCTACAGACTGC-3'; R: 5'-CATCCTGGAGATTCTCTACCACT-3', β-actin F: 5'-CAGTACGTTGCTATCCAGGC-3'; R: 5'-CTCCTTAATGTCACGCACGAT-3', Hsa-miR-93-3p 5': ACTGCTGAGCTAGCACTTCC.

Plasmid and Transfection

The human pCMV3-DAPK1 (Sino Biological, Beijing, China) plasmids and dual-luciferase reporter plasmids (GenePharma Corporation, Suzhou, Jiangsu, China) were transfected with P3000™reagents and Lipofectamine™ 3000 transfection reagent (Invitrogen, Carlsbad, CA, USA), and operated strictly according to instruction.

The two most effective STAT3 siRNAs, agomir, antagomir, and their negative control (GenePharma Corporation, Suzhou, Jiangsu, China), were transfected with

lipofectamine^{TM} 3000 transfection reagent. The siRNA sequences were as follows: si-STAT3-1 5'-CAUCUGCCUAGAUCGGCUAdtdt-3'; 5'-UAGCCGAUCUAGGCAGAUGdtdt-3', si-STAT3-2 5'-GCAGGAUCUAGAACAGAATT-3'; 5'-UUUCUGUUCUAGAUCCUGCTT-3'.

Lentivirus vector transduction

Cells were transduced with STAT3-overexpressed lentiviruses (GenePharma Corporation, Suzhou, Jiangsu, China) in complete medium containing 5 μg/ml polybrene and incubated at 37°C in 5% CO_2. Cells were culture for 48 hours and harvested for detecting of transduction efficiency by qRT-PCR, and GFP expression was observed by fluorescence microscopy 72 hours after transduction,

Xenograft tumor model and staining

BALB/c nude mice (4-week-old, 14–16 g, female) were purchased from Beijing Vital River Experimental Animal Technology Co Ltd, housed in barrier facilities on a 12h light/dark cycle. The Institutional Animal Care and Use Committee of China Medical University supervised and approved all of the experimental procedures. Overexpressed miR-93-3p ACHN cells and negative control cells ($4\text{-}6\times10^6$) were inoculated subcutaneously in the left dorsal flanks. The length and width were measured with calipers, and tumor volumes were calculated using the equation (Length × Width^2)/2. The volume of xenograft tumors was recorded every week. On the 45th day, the animals were euthanized, and the tumors were excised, weighed, and paraffin-embedded. Serial 6.0μm sections were cut and subjected to staining assays. The proportion of Ki-67 (Abcam, Cambridge, MA, USA) stained cells was counted and determined to assess the proliferative capacity. Apoptosis was assayed by the DeadEnd Fluorimetric TUNEL system (Promega, Beijing, China).

Western blotting

Cultured cells were washed, harvested, and lysed on the ice of RIPA lysis buffer containing Protease Inhibitor Cocktail and Phosphatase Inhibitor Cocktail (1:100, Bimake, 9330 Kirby Drive, STE 200, Houston, TX, USA). Rabbit monoclonal primary antibodies were specific to DAPK1, STAT3, pSTAT3 (Cell Signaling Technology, Danvers, MA, USA), GAPDH (Sigma-Aldrich, MO, USA), Histone H3 (Abcam, Cambridge, MA, USA). Following washing with TBST, the membranes were incubated with secondary antibodies to rabbit IgG (1:5000, ZSBG-BIO, Beijing, China). The densitometry values were calculated with Image J software. Nuclear extracts were obtained with a Nuclear Extraction Kit (Abcam, Cambridge, MA, USA) according to the manufacturer's protocol.

Cell proliferation and viability assay

Cells were seeded before treatment, and Cell Counting Kit-8 assay (CCK-8, Dojindo Molecular Technologies, Inc. Shanghai, China) was used to assess the proliferation potential. Each assay was repeated at least 3 times. Three replicates were made for each time point.

Cell apoptosis assay

Cell apoptosis was examined using flow-cytometry analysis, performed using a FACSCalibur flow cytometer (Becton Dickinson Biosciences, San Jose, CA) equipped with CellQuest software (BD Biosciences). The cells were collected and stained with FITC Annexing V and PI (Pharmingen Annexin V FITC Apoptosis Kits, BD, San Diego, CA, USA).

IL-6 and Stattic treatment

IL-6 (Sino Biological, Beijing, China) and Stattic (Selleck, Shanghai, China) were reconstituted according to the manufacturer's protocol. Before treatment, cells were cultured with serum-free medium for 12 hours. IL-6 and stattic solution was diluted in serum-free medium to the different concentration. Serum-free medium was used in the control group.

Immunofluorescence

Immunofluorescence images were captured with an inverted fluorescence microscope (Olympus, Tokyo, Japan). After transfection, cells were seeded in 24-well plates and treated with IL-6 at 20 ng/ml for 20 mins. Then, cells were reacted with rabbit polyclonal antibody against pSTAT3 (1:200, Cell Signaling Technology, Danvers, MA, USA) in blocking buffer overnight. Before viewing, the nuclei were stained with DAPI (Beyotime, Shenzhen, Guangdong, China).

Chromatin immunoprecipitation assay

The chromatin immunoprecipitation (ChIP) assay was performed using SimpleChIP® Plus Sonication Chromatin IP Kit (Cell Signaling Technology, Danvers, MA, USA) according to the manufacturer's protocol. After reverse cross-linking by heating at 60°C and vibrating for more than 2 hours, qRT-PCR was performed using promoter-specific forward and reverse primers, as follows: F: 5'-AAAACAAATTCCACGCTCCT-3'; R: 5'-GCTCTGCCACTTCCTCACA-3'. Precipitated DNA was also amplified for 25 cycles and was resolved on 2% agarose gel to evaluate the target DNA.

Statistical analysis

Each experiment was repeated three times. All statistical analyses were carried out using SPSS 21.0 statistical software (SPSS Inc., Chicago, IL, USA), and the results are presented as the mean ± SD. The 2-tailed Student's t-test was used to evaluate the significance of differences between two groups of data in all pertinent experiments. Mann–Whitney U test was performed for unpaired group comparisons. A p-value < 0.05 was considered significant.

Results

miR-93-3p was up-regulated in RCC tissues and cell lines

First, we assessed the expression levels of miR-93-3p in RCC tissues using online public data from the Cancer Genome Atlas (TCGA). We found that miR-93-3p expression levels were significantly up-regulated in RCC tissues compared with normal tissues (Supplementary Figure a). Furthermore, miR-93-3p expression levels were qualified in 96 paired RCC samples and adjacent normal tissues using qRT-PCR, and normalized to GAPDH ($P<0.05$; Figure 1a). The results were consistent with the TCGA data analysis. What's more, we assessed the expression of miR-93-3p in RCC cell lines (ACHN, 786-O, 760-P, OSRC-2, CAKI-1), and in a normal tubular epithelial cell line (HK-2). The expression of miR-93-3p was also found to be elevated in all of the RCC cell lines compared with the normal cell line ($P<0.05$; Figure 1b).

miR-93-3p increased RCC cells proliferation in vitro and enhanced tumor growth in vivo

To investigate the function of miR-93-3p in tumors' development and progression, RCC cell lines, ACHN and 786-O, were transfected with the agomir and antagomir of miR-93. After transfection, we performed colony formation assays and CCK-8 assays to evaluate the function of miR-93-3p on cell proliferation and viability. Over-expression of miR-93-3p increased the proliferation and viability rates of RCC cells, while inhibition of miR-93-3p expression suppressed cell proliferation and viability ($P<0.05$; Figure 1c and 1d).

To examine the effects of miR-93-3p on the progression of RCC in vivo, nude mice were subcutaneously inoculated with ACHN cells. After cells transfected with agomir of miR-93-3p and negative control were injected intratumorally, two groups were backed into cages to continue to be raised for 45 days. The results showed that the tumors, received an agomir injection grew much faster than the tumors from negative control groups (Figure 1e). The size of xenograft tumors in agomir groups were significantly smaller compared with that in the control group. The further histological examination showed that the miR-93 over-expression groups increased the expression of Ki67 in xenograft tumor cells compared with the control groups (Figure 1f). These results further confirmed that up-regulated miR-93 enhanced tumor growth in vivo and in vitro.

miR-93 mediated RCC cells apoptosis by inhibiting DAPK1 expression

To evaluate the effect of miR-93 on the apoptosis of RCC in vitro, flow cytometry analysis was performed. The proportion of apoptotic cells transfected with miR-93 agomir significantly decreased compared with the negative control group, while inhibition of miR-93 expression promotes cell apoptosis ($P<0.05$, Figure 2a).

Moreover, TUNEL Assays showed that in vivo, the apoptotic cells, marked as green spots, in agomir groups were less than the negative control group (Figure 2b).

Next, we explored the potential targets of miR-93 by miRWalk 2.0 (http://diana.imis.athena-innovation.gr/DianaTools/index.php?r=microT_CDS/index) and found that death-associated protein kinase 1, DAPK1, was a putative target of miR-93-3p (Figure 2c). Next, we investigated whether miR-93 could regulate specifically the expression of DAPK1 through qRT-PCR and western blotting. Western blotting confirmed that in the cells transfected with agomir, up-regulated miR-93 significantly decreased and protein levels of DAPK1, while the cells transfected with antagomir showed the opposite result in the two RCC cell lines ($P<0.05$, Figure 2d). However, there were no differences among each transfection groups from the results of qRT-PCR (ns $P>0.05$, Supplemental Figure b). That indicates miR-93 might impact on the protein levels of DAPK1, but it would have no effects on mRNA levels of DAPK1. Then, the dual-luciferase reporter assay was performed to examine miR-93 directly bound with the 3′UTR region of DAPK1 mRNA. According to the predicted binding site, we structured and co-transfected pmirGLO luciferase reporter plasmids, respectively containing a wild-type and a mutant-type DAPK1 3′UTR, with miR-93 agomir or negative control in 293T cells. The data from the ration of absorbance showed that luciferase activity of the cells transfected with wild-type plasmid and agomir was down-regulated. In contrast, there was no significant change when the cells were transfected with the mutant type. ($P<0.05$, Figure 2e). After that, we performed the recovery assay by western blotting to further verify miR-93 regulate the protein expression of DAPK1 (Figure 2f). CCK-8 and apoptosis recovery assay were also examined among mock, miR-93, DAPK1 and recovery groups (Figure 2g and 2h).

STAT3 induced miR-93 expression

We further investigated whether miR-93 regulation was related to some crucial signaling pathways involved in cancer development or progression. First, we searched miR-93 gene using UCSC Genome Browse website (http://genome.ucsc.edu/). We selected upstream by 2000 bases and downstream by 1000 bases, and got the promoter region sequence of miR-93. Then, we typed the sequence into Jaspar (http:// jaspar.genereg.net/) and Promoter Scan (http:// www-bimas.cit.nih.gov/molbio/proscan/) search term, set threshold score 90% and got a series of transcription factors and their bound sites. Bioinformatics data indicated that there was one STAT3 bound site within the miR-93 promoter, which matched each other from the two websites (Figure 3a). To verify this finding, we measured the expression of miR-93-3p and STAT3 in 96 RCC samples, and we found there was a positive correlation between the expression of the two factors ($P<0.05$, $R^2=0.41$, Figure 3b). Then the expression of miR-93-3p was quantified by qRT-PCR in ACHN and 786-O cells under two adverse stimuluses. Above all, we examined Interleukin 6 (IL-6) as an exogenous activator of STAT3, and stattic as an exogenous inhibitor by western blotting. Then, we measured the concentration-pSTAT3 curve and time-pSTAT3 curve of activator and inhibitor by western blotting. 786-O cell lines were treated at different concentrations of 10μg/ml, 20 μg/ml, 30 μg/ml and 40 μg/ml IL-6 solution for 20 mins. The value of pSTAT3, active STAT3, from 20 μg/ml, 30 μg/ml and, 40 μg/ml group exhibited stronger than 10 μg group, and there was no significant difference among the last three groups. Since adding 20 μg/ml IL-6 solution for 10 mins, pSTAT3 began to ascend, until 20 mins, the account of pSTAT3 peaked to twice as free serum medium group. Last, we found the expression of both miR-93-3p was up-regulated in 786-O cells treated with 20ng/ml IL-6, while the expression

showed the opposite tendency under 20μM stattic stimulating (Figure 3c). Interestingly, we found the expression of miR-93-3p rose 30 mins later, and it reached the highest peak value after 2-hour-treatment (Figure 3d). For 6 hours under IL-6 continuously stimulating, the expression of miR-93-3p decreased. Furthermore, we next directly knocked down STAT3 by transfecting two silence interfere RNAs (siRNA) of STAT3, performed qRT-PCR to examine the change of miR-93-3p. Consistent with exogenous cytokine regulation, miR-93 expression was found to be significantly decreased when transfection with siRNA (Figure 3e). These results demonstrated that the activation of STAT3 induced miR-93 expression, whereas the inhibition of STAT3 signaling suppressed miR-93 expression.

STAT3 directly bound the promoter region of the miR-93

To verify the direct binding of STAT3 at the predicted potential sites in the promoter region of miR-93, pmirGLO luciferase reporter plasmids, containing miR-93 promoter sequence and corresponding mutant sequence, were constructed (Figure 4a). After transfection with Mut and WT plasmids, cells continued to culture for 36 hours, and treated with 20 ng/ml solution and free serum medium for 2 hours. Then we washed the four groups' cells and performed the next luciferase reporter assay. Dual-luciferase reporter assays emerged that IL-6 treatment significantly increased the luciferase activity in the cells transfected with the wild-type plasmids (Figure 4b). Furthermore, the chromatin immunoprecipitation (ChIP) assay revealed that activated STAT3 bound with the promoter sequence of the miR-93, then the results were verified through qRT-PCR and DNA-agarose gel electrophoresis (Figure 4c and 4d). These data strongly supported that STAT3 directly induced miR-93 by enhancing its transcription expression.

DAPK1 and STAT3 interact on each other to regulate cell apoptosis and proliferation

In the previous study, knockdown of DAPK1 attenuated the curcumin-induced G2/M cell cycle arrest and apoptosis by modulating STAT3 in GBM cells [15]. We further investigated whether it would exist the uncover regulatory mechanism between STAT3 and DAPK1 in RCC. We assessed the expression of DAPK1 in 786-O and ACHN cells transfected with siRNA of STAT3 by qRT-PCR and western blotting, and expression under stattic stimulating (Figure 5a, 5b and, 5c). The results presented that both protein and mRNA expression levels were down-regulated in exogenous cytokine stimulation and RNA interference cells. It demonstrated that STAT3, as an oncogenic transcription factor, might regulate DAPK1 mRNA and protein expression in RCC. However, there was no difference on protein and mRNA expression levels of STAT3 in RCC cells transfected with pcDNA-DAPK1 (Supplemental figure c and d). However, pSTAT3 in the nucleus of cells transfected with plasmids decreased significantly compared with negative control groups (Figure 5d). Moreover, the account of pSTAT3 entry into nucleus descended under each view in immunofluorescence assay after RCC cells were transfected with plasmids compared with RCC cells transfected with negative control (Figure 5e). We found that under high power fields in DAPK1 over-expressed group, a highlight cycle-bond around the nucleus, which might be from accumulated pSTAT3 owing to the prevention of DAPK1, while it disappeared in double treatment group. Thus, DAPK attenuated STAT3 transcriptional activity by decreasing pSTAT3 entry into nuclear. Alternatively, inactivation or activated of STAT3 led to an increase or decrease in DAPK mRNA and protein levels.

Discussion

Early diagnosis plays a crucial role in RCC treatment. Hence, the high specificity and high sensitivity diagnosis biomarker of RCC is necessary and urgent. In this study, we identified miR-93-3p as an onco-miRNA role, involved in apoptosis and proliferation of RCC, and we revealed a potential regulation pathway of STAT3/miR-93-3p/DAPK1. Our data demonstrated that activated STAT3 promotes miR-93-3p expression by binding to promoter region, then miR-93-3p suppressed the protein level of DAPK1 in RCC cells. What's more, DAPK1 mediates the activation of STAT3 pathway through blocking pSTAT3 translation into the nucleus. That constructs a feedback regulation loop. Moreover, STAT3, as a transcriptional factor, induced the protein and mRNA expression of DAPK1, suggesting STAT3 might directly regulate DAPK1, not just impact mRNA of DAPK1 by miR-93-3p (Figure 6).

Death-associated protein kinase 1, DAPK1, a Ca2+/calmodulin (CaM)-dependent serine/threonine-protein kinase, plays an important role in diverse apoptosis, autophagy pathways and immune responses of autoimmune disorders, neurodegenerative diseases, ischemic damage and many types of cancer. Several mechanisms account for DAPK deregulation in cancer, including transcriptional and post-transcriptional regulation. The 5'-UTR of the DAPK1 gene contains CpG islands. Hyper-methylation of DAPK1 in CpG islands has been detected in many tumors, leading to gene silencing [16]. The expression of DAPK1 is correlated with p53 activation in both normal and cancer cells in response to DNA damage. EMSA and Chromatin-IP assays revealed nine p53 could bind with upstream of the first exon or within the first intron of DAPK and confirmed p53 could positively regulate DAPK1 expression [17]. Except for p53, ERK could control DAPK1 by

phosphorylating DAPK1 at Ser735 leading to DAPK1 activity, which trigger further DAPK-ERK interaction through their death domains, finally promote cell apoptosis [18]. UNC5B interacts with DAPK1 through their death domains to act its pro-apoptotic function. What's more, UNC5B activates DAPK1 by inhibiting DAPK auto-phosphorylation at Ser308 [19]. On the mRNA level, DAPK1 down-regulation can also be mediated by microRNA -dependent mechanism. MiR-103/107 could target DAPK 3'-UTR to interfere with translation and promote metastasis in colorectal cancer [20]. On the other hand, post-translational regulation includes protein phosphorylation by other kinases, auto-phosphorylation of S308, ubiquitination [21], and protease-mediated degradation. STAT3 is one of the angiogenesis-related transcription factors, related to RCC proliferation, migration, and survival [22-24]. However, it is unclear that STAT3 interacts with DAPK1 in RCC. In this study, we regulated expression or activation of STAT3 by overexpression plasmids and exogenous activator in RCC cell lines, and dramatically found that the mRNA and protein expression of DAPK1 was regulated in contrast with that of STAT3. It demonstrated that STAT3 activation and up-regulation might transcriptionally repress DAPK1. The preview report shows that DAPK mRNA level is negatively regulated via the non-canonical Flt3lTD/NF-κB pathway [25]. But there was no reports related to STAT3 as a transcription factor, targeted to DAPK1. Then we searched bio-information websites to verify whether STAT3 could bind to the promoter region of DAPK1. The sequence analysis of the DAPK promoter (Database of Transcriptional StartSites: DBTSS: NM_004938) and UCSC Genome Browser revealed that the scheme of the DAPK promoter illustrated two putative STAT3 binding sites, region 1(-1471 to -1821) and region 2 (-351 to -631). The preview findings identified that the suppressive function of DAPK1 suppress the pathway of

TCR- and LPS-triggered NF-κB activation [26]. Lungs and macrophages of DAPK1 knockdown mice secreted higher levels of IL-6 and CXCL1 in response to LPS [27]. Thus, DAPK1 could inhibit activation of the inflammatory cytokines and suppress the progress of inflammatory reaction. Abnormal activation of inflammatory cytokines also plays important roles in tumorigenesis, progression, invasion, and metastasis. We assumed whether DAPK1 affect inflammatory pathways, which STAT3 or pSTAT3 was involved. Furthermore, we up-regulated expression of DAPK1 by transfecting plasmids, and found there were no changes on neither mRNA nor protein expression level of STAT3. However, interestingly, the expression of miR-93-3p, as downstream of STAT3, was increased. We though whether DAPK1 affected the activation of STAT3 or the transportation of pSTAT3. We performed Immunofluorescence and examined the protein level of pSTAT3 in nuclear. The results demonstrated that the progress of pSTAT3 transportation was suppressed by the raise of DAPK1 in RCC cells. To sum up, activated STAT3 might be enriched in the DAPK promoter sequence and repressive the transcription progress of DAPK1.On the other hand, DAPK might act as a negative regulator of STAT3, attenuate the activity of STAT3 through preventing STAT3 nuclear localization pathway. How did DAPK1 de-activate STAT3? We considered there might be two reasons, the first is that DAPK1 would impact protein conformation of activated STAT3 via protein-protein interaction. It led to dimerization of pSTAT3, the functional STAT3 structure, prevented out of the nucleus. However, we performed Co-IP assays, which showed there were no direct constitution with pSTAT3 and DAPK1 (Supplemental Figure e). The second is that DAPK1 inhibit the upstream inflammatory factors, which could activate STAT3 or translocate STAT3 to the nucleus, such as IL-6, TNF-α and, IFN-γ. The important implication of this study that DAPK1 and STAT3 negatively

regulate each other in RCC cell lines, what's more, STAT3 promotes miR-93 to suppress the pro-apoptosis and anti-proliferation function of DAPK1. This finding opens a novel pathway between tumorigenesis and inflammatory reaction. Moreover, it offers a new therapeutic perspective for the treatment of renal cell carcinoma.

Conclusions

In summary, we revealed that miR-93-3p act an oncogene in renal cell carcinoma, enhanced cell proliferation, and suppressed apoptosis. It was directly regulated by STAT3 and inhibited DAPK1 protein-expression. In addition, DAPK1 inactivated STAT3, and STAT3 decreased the expression of DAPK1. We hope to provide a new study view about STAT3/miR-93-3p/DAPK1 signalling feedback pathway involved in inflammatory reaction and cancer. Therefore, disrupting this pathway might be a promising therapeutic approach in the treatment of renal cell carcinoma.

Author contribution

YD designed, performed the experiments, organized data and wrote the paper. CK acquired funding, established the urology laboratory, provided the required equipment and instruments, supervised assays, contributed to the critical reading of the manuscript, generated the figures, and gave final approval of the manuscript.

Acknowledgements

We are particularly grateful to Pro.Xueshan Qiu for his timely help.

Fundings

This work was supported by Shenyang Plan Project of Science and Technology (Grant No. F19-112-4-098), National key R & D plan key research projects of precision medicine (2017YFC0908000), China Medical University's 2018 discipline promotion program. The authors declare no competing financial interests. Funding agency did not participate in the design of the study and collection, analysis and interpretation of data and in writing the manuscript.

Conflict of Interest

The authors declare that they have no conflict of interest.

Abbreviations

RCC renal cell carcinoma

TCGA the Cancer Genome Atlas

TUNEL terminal deoxynucleotidyl transferase dUTP nick end labeling

Reference

1. Rini BI, Campbell SC, Escudier B: **Renal cell carcinoma**. *Lancet* 2009, **373**(9669):1119-1132.
2. Chen W, Zheng R, Baade PD, Zhang S, Zeng H, Bray F, Jemal A, Yu XQ, He J: **Cancer statistics in China, 2015**. *CA Cancer J Clin* 2016, **66**(2):115-132.
3. Capitanio U, Montorsi F: **Renal cancer**. *Lancet* 2016, **387**(10021):894-906.
4. Beitzinger M, Meister G: **Preview. MicroRNAs: from decay to decoy**. *Cell* 2010, **140**(5):612-614.
5. Di Leva G, Garofalo M, Croce CM: **MicroRNAs in cancer**. *Annu Rev Pathol* 2014, **9**:287-314.
6. Hammond SM: **An overview of microRNAs**. *Adv Drug Deliv Rev* 2015, **87**:3-14.
7. Medina PP, Slack FJ: **microRNAs and cancer: an overview**. *Cell Cycle* 2008, **7**(16):2485-2492.
8. Mohr AM, Mott JL: **Overview of microRNA biology**. *Semin Liver Dis* 2015, **35**(1):3-11.

9. Liu Y, Zhang Y, Wen J, Liu L, Zhai X, Liu J, Pan S, Chen J, Shen H, Hu Z: **A genetic variant in the promoter region of miR-106b-25 cluster and risk of HBV infection and hepatocellular carcinoma**. *PLoS One* 2012, **7**(2):e32230.
10. Lo Sardo F, Forcato M, Sacconi A, Capaci V, Zanconato F, Di Agostino S, Del Sal G, Pandolfi PP, Strano S, Bicciato S *et al*: **MCM7 and its hosted miR-25, 93 and 106b cluster elicit YAP/TAZ oncogenic activity in lung cancer**. *Carcinogenesis* 2017, **38**(1):64-75.
11. Cioffi M, Vallespinos-Serrano M, Trabulo SM, Fernandez-Marcos PJ, Firment AN, Vazquez BN, Vieira CR, Mulero F, Camara JA, Cronin UP *et al*: **MiR-93 Controls Adiposity via Inhibition of Sirt7 and Tbx3**. *Cell Rep* 2015, **12**(10):1594-1605.
12. Espinosa-Parrilla Y, Munoz X, Bonet C, Garcia N, Vencesla A, Yiannakouris N, Naccarati A, Sieri S, Panico S, Huerta JM *et al*: **Genetic association of gastric cancer with miRNA clusters including the cancer-related genes MIR29, MIR25, MIR93 and MIR106: results from the EPIC-EURGAST study**. *Int J Cancer* 2014, **135**(9):2065-2076.
13. Wang L, Wang Q, Li HL, Han LY: **Expression of MiR200a, miR93, metastasis-related gene RECK and MMP2/MMP9 in human cervical carcinoma--relationship with prognosis**. *Asian Pac J Cancer Prev* 2013, **14**(3):2113-2118.
14. Otsuka M, Jing Q, Georgel P, New L, Chen J, Mols J, Kang YJ, Jiang Z, Du X, Cook R *et al*: **Hypersusceptibility to vesicular stomatitis virus infection in Dicer1-deficient mice is due to impaired miR24 and miR93 expression**. *Immunity* 2007, **27**(1):123-134.
15. Wu B, Yao H, Wang S, Xu R: **DAPK1 modulates a curcumin-induced G2/M arrest and apoptosis by regulating STAT3, NF-kappaB, and caspase-3 activation**. *Biochem Biophys Res Commun* 2013, **434**(1):75-80.
16. Pulling LC, Grimes MJ, Damiani LA, Juri DE, Do K, Tellez CS, Belinsky SA: **Dual promoter regulation of death-associated protein kinase gene leads to differentially silenced transcripts by methylation in cancer**. *Carcinogenesis* 2009, **30**(12):2023-2030.
17. Martoriati A, Doumont G, Alcalay M, Bellefroid E, Pelicci PG, Marine JC: **dapk1, encoding an activator of a p19ARF-p53-mediated apoptotic checkpoint, is a transcription target of p53**. *Oncogene* 2005, **24**(8):1461-1466.
18. Chen CH, Wang WJ, Kuo JC, Tsai HC, Lin JR, Chang ZF, Chen RH: **Bidirectional signals transduced by DAPK-ERK interaction promote the apoptotic effect of DAPK**. *EMBO J* 2005, **24**(2):294-304.

19. Llambi F, Lourenco FC, Gozuacik D, Guix C, Pays L, Del Rio G, Kimchi A, Mehlen P: **The dependence receptor UNC5H2 mediates apoptosis through DAP-kinase**. *EMBO J* 2005, **24**(6):1192-1201.
20. Chen HY, Lin YM, Chung HC, Lang YD, Lin CJ, Huang J, Wang WC, Lin FM, Chen Z, Huang HD *et al*: **miR-103/107 promote metastasis of colorectal cancer by targeting the metastasis suppressors DAPK and KLF4**. *Cancer Res* 2012, **72**(14):3631-3641.
21. Jin Y, Blue EK, Dixon S, Shao Z, Gallagher PJ: **A death-associated protein kinase (DAPK)-interacting protein, DIP-1, is an E3 ubiquitin ligase that promotes tumor necrosis factor-induced apoptosis and regulates the cellular levels of DAPK**. *J Biol Chem* 2002, **277**(49):46980-46986.
22. Guo C, Yang G, Khun K, Kong X, Levy D, Lee P, Melamed J: **Activation of Stat3 in renal tumors**. *Am J Transl Res* 2009, **1**(3):283-290.
23. Horiguchi A, Oya M, Marumo K, Murai M: **STAT3, but not ERKs, mediates the IL-6-induced proliferation of renal cancer cells, ACHN and 769P**. *Kidney Int* 2002, **61**(3):926-938.
24. Horiguchi A, Oya M, Shimada T, Uchida A, Marumo K, Murai M: **Activation of signal transducer and activator of transcription 3 in renal cell carcinoma: a study of incidence and its association with pathological features and clinical outcome**. *J Urol* 2002, **168**(2):762-765.
25. Shanmugam R, Gade P, Wilson-Weekes A, Sayar H, Suvannasankha A, Goswami C, Li L, Gupta S, Cardoso AA, Baghdadi TA *et al*: **A noncanonical Flt3ITD/NF-kappaB signaling pathway represses DAPK1 in acute myeloid leukemia**. *Clin Cancer Res* 2012, **18**(2):360-369.
26. Chuang YT, Fang LW, Lin-Feng MH, Chen RH, Lai MZ: **The tumor suppressor death-associated protein kinase targets to TCR-stimulated NF-kappa B activation**. *J Immunol* 2008, **180**(5):3238-3249.
27. Nakav S, Cohen S, Feigelson SW, Bialik S, Shoseyov D, Kimchi A, Alon R: **Tumor suppressor death-associated protein kinase attenuates inflammatory responses in the lung**. *Am J Respir Cell Mol Biol* 2012, **46**(3):313-322.

Figure legends

Figure 1, miR-93 promoted RCC cells proliferation in vivo and vitro.

Figure 1a, Relative expression of miR-93-3p in 96 pairs of renal cell carcinoma and adjacent normal tissues.

Figure1 b, Relative expression of miR-93-3p in RCC cell lines and normal kidney proximal tubule epithelial cell line.

Figure 1c, d and e, Proliferation assays in vitro and vivo.

Figure 1f, The Ki67 immuno-staining cell in the xenograft tumor.

Figure 2, miR-93 suppressed the protein level of DAPK1 to down-regulated RCC cells apoptosis.

Figure 2a, The apoptosis cell count calculated by flow cytometer different groups.

Figure 2b, The apoptosis cells marked with red arrows in the xenograft tumor shown by Tunel assays.

Figure 2c, The highly conserved DAPK1 3′UTR and predicted miR-93-3p target

sequence in the 3′UTR of DAPK1 and the mutant type with 8 altered nucleotides.

Figure 2d, Overexpression of miR-93-3p significantly decreased protein levels of DAPK1.

Figure 2e, The luciferase assay was performed with co-transfection of miR-93-3p and wild-type or mutant-type DAPK1 3′UTR. Firefly luciferase activity of each sample was normalized against renilla luciferase activity.

Figure 2f, g, and h, The recovery assays confirmed miR-93-3p promoted proliferation and inhibited apoptosis by mediating DAPK1.

Figure 3, STAT3 up-regulated the expression miR-93.

Figure 3a, Schematic of miR-93 promoter. The predicted STAT3 binding sites were located at -1736 to -1746.

Figure 3b, The correlation between the expression of STAT3 and miR-93.

Figure 3c, The optimum concentration and effective time range of the activator and inhibitor of STAT3. IL6 and Stattic launched their effect after added in 20 mins.

Figure 3d, The time-miR93 curve after 786-O cells treated under 20ng/ml and 20μM Stattic.

Figure 3e, Relative expression of miR-93-3p in siRNA treated cells.

Figure 4, STAT3, as a transcripiton factor, bound with the promoter region of miR-93.

Figure 4a, miR-93 promoter region was cloned into a pmirGLO luciferase reporter plasmid. For the mutant type, 10 nucleotides at the predicted binding site were altered simultaneously.

Figure 4b, Luciferase assay results showed that activation of STAT3 significantly increased the luciferase activity in cells transfected with luciferase reporter plasmid containing the wild-type miR-93 promoter.

Figure 4c, qRT-PCR was also performed to measure the enrichment of predicted binding fragments.

Figure 4d, ChIP assay results showed that STAT3 physically bound with the miR-93 promoter. Lane 1, input chromatin prior to IP. Lane 2, IP with the non-specific antibody, IgG. Lane 3, IP with pSTAT3 antibody when IL6-stimulating. Lane 4, IP with just pSTAT3.

Figure 5, STAT3 inhibited the mRNA and protein level of DAPK1, and DAPK1 deactivated STAT3.

Figure 5a, Relative expression of DAPK1 measured in qRT-PCR after two cell lines treated by siRNA.

Figure 5b, Relative expression of DAPK1 measured in qRT-PCR when STAT3 inactivation.

Figure 5c, The protein expression of DAPK1 among different groups with STAT3 knockdown and inactivation.

Figure 5d, pSTAT3 in nuclear proteins extracted were measured by western blot analysis.

Figure 5e, Immunofluorescence assay showed that DAPK1 attenuated pSTAT3 entry into nuclear.

Figure 6, STAT3 regulates miR93-mediated apoptosis through inhibiting DAPK1 in Renal cell carcinoma. STAT3 promotes miR-93-3p expression by binding to promoter region, then miR-93-3p suppressed DAPK1. What's more, DAPK1 mediates the activation of STAT3 pathway through blocking pSTAT3 translation into the nucleus, and STAT3 decreased the expression of DAPK1.

Supplemental figure a, Relative expression of miR-93 in renal cell carcinoma tissue and adjacent normal tissue from the TCGA KIRC miRNA database.

Supplemental figure b, Relative expression of DAPK1 measured by qRT-PCR among miR-93 hypo- and hyper-expression groups.

Supplemental figure c, Relative mRNA expression of STAT3 measured by qRT-PCR after DAPK1 up-regulated.

Supplemental figure d, Relative protein expression of STAT3 measured by western blotting after DAPK1 up-regulated.

Supplemental figure e, DAPK1-pSTAT3 Co-IP assays showed there was no direct constitution with pSTAT3 and DAPK1.

Figures

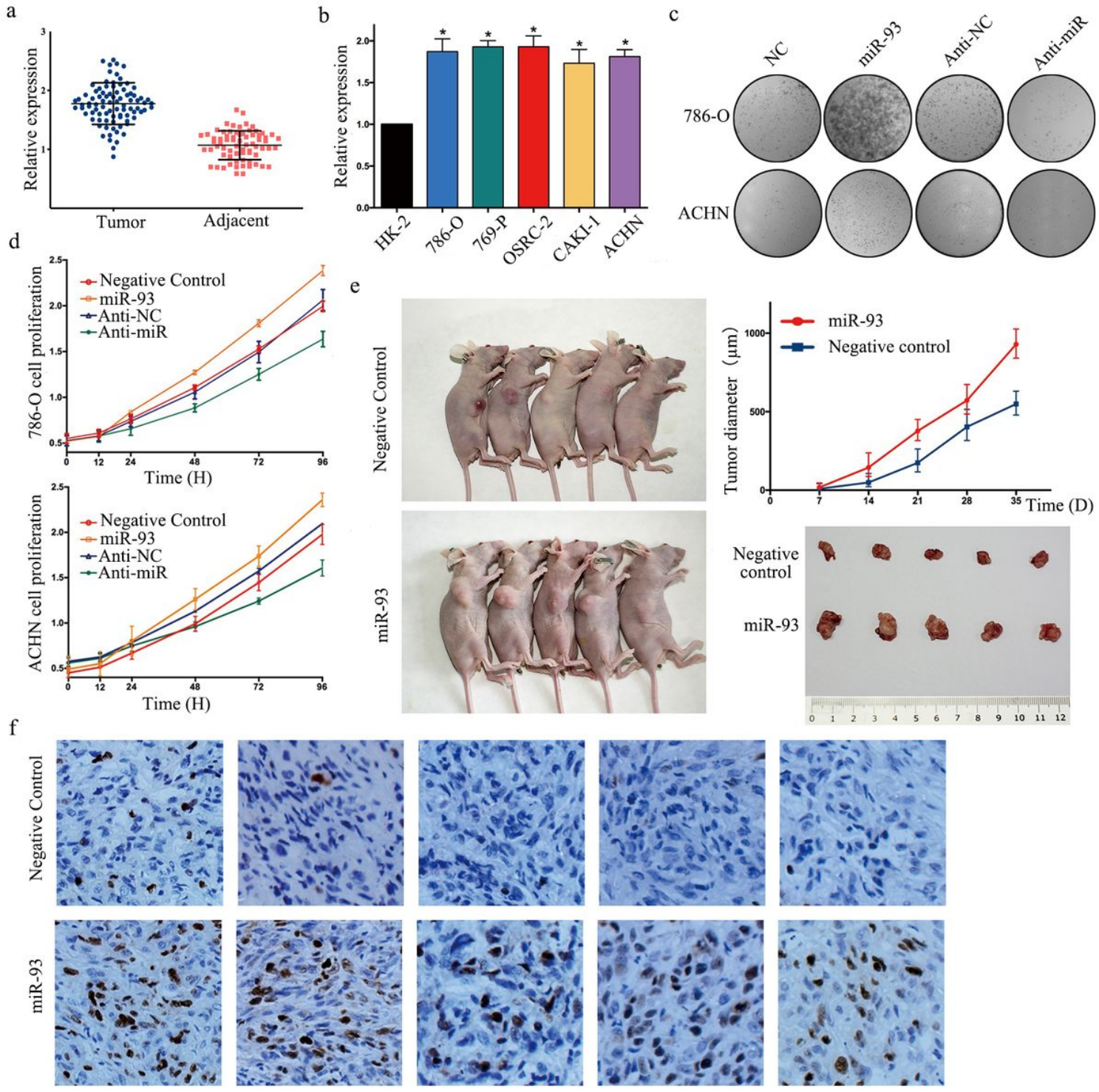

Figure 1

miR-93 promoted RCC cells proliferation in vivo and vitro. a, Relative expression of miR-93-3p in 96 pairs of renal cell carcinoma and adjacent normal tissues. b, Relative expression of miR-93-3p in RCC cell lines and normal kidney proximal tubule epithelial cell line. c, d and e, Proliferation assays in vitro and vivo. f, The Ki67 immuno-staining cell in the xenograft tumor.

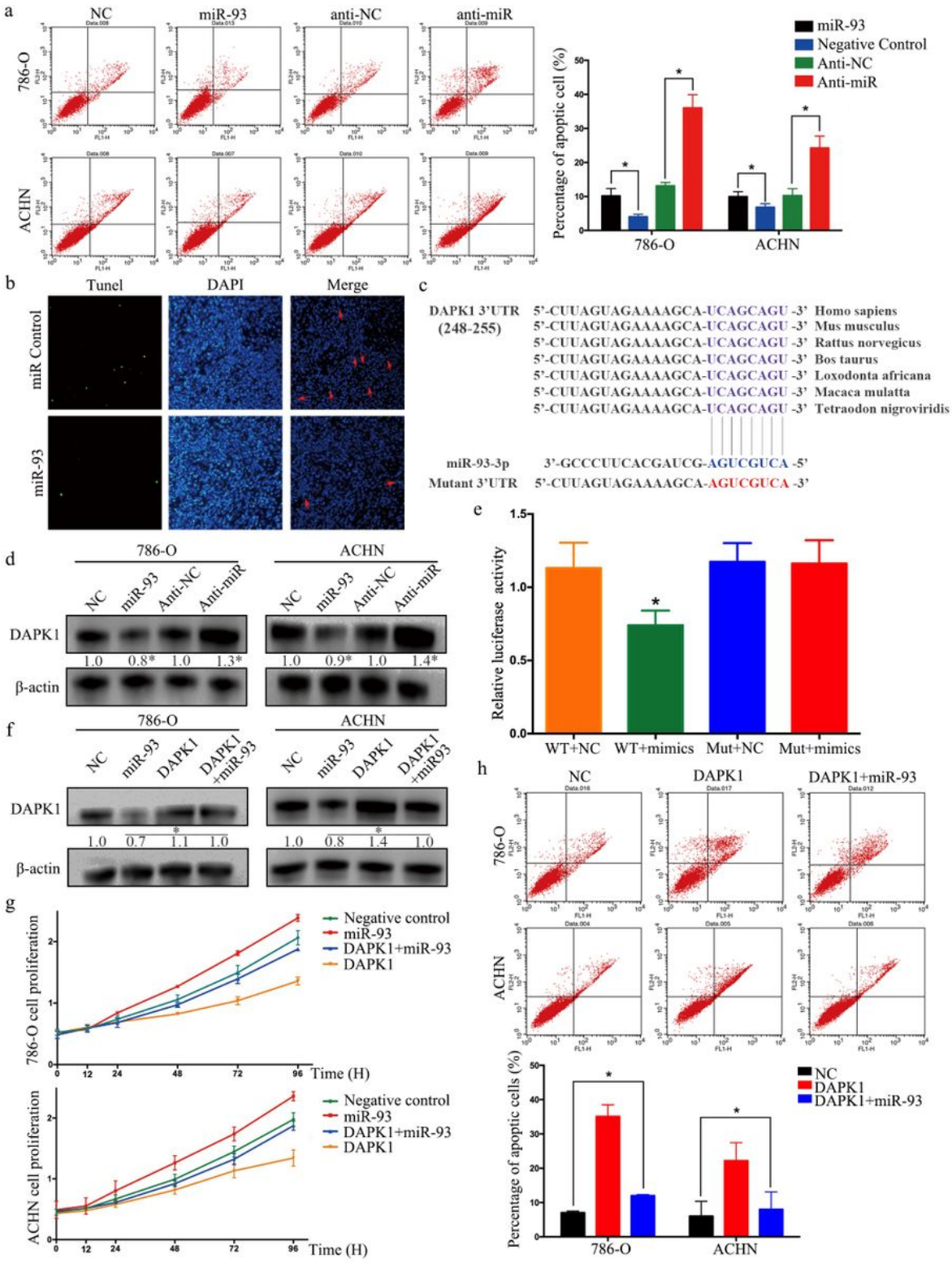

Figure 2

miR-93 suppressed the protein level of DAPK1 to down-regulated RCC cells apoptosis. a, The apoptosis cell count calculated by flow cytometer different groups. b, The apoptosis cells marked with red arrows in the xenograft tumor shown by Tunel assays. c, The highly conserved DAPK1 3'UTR and predicted miR-93-3p target sequence in the 3'UTR of DAPK1 and the mutant type with 8 altered nucleotides. d, Overexpression of miR-93-3p significantly decreased protein levels of DAPK1. e, The luciferase assay was

performed with co-transfection of miR-93-3p and wild-type or mutant-type DAPK1 3'UTR. Firefly luciferase activity of each sample was normalized against renilla luciferase activity. f, g, and h, The recovery assays confirmed miR-93-3p promoted proliferation and inhibited apoptosis by mediating DAPK1.

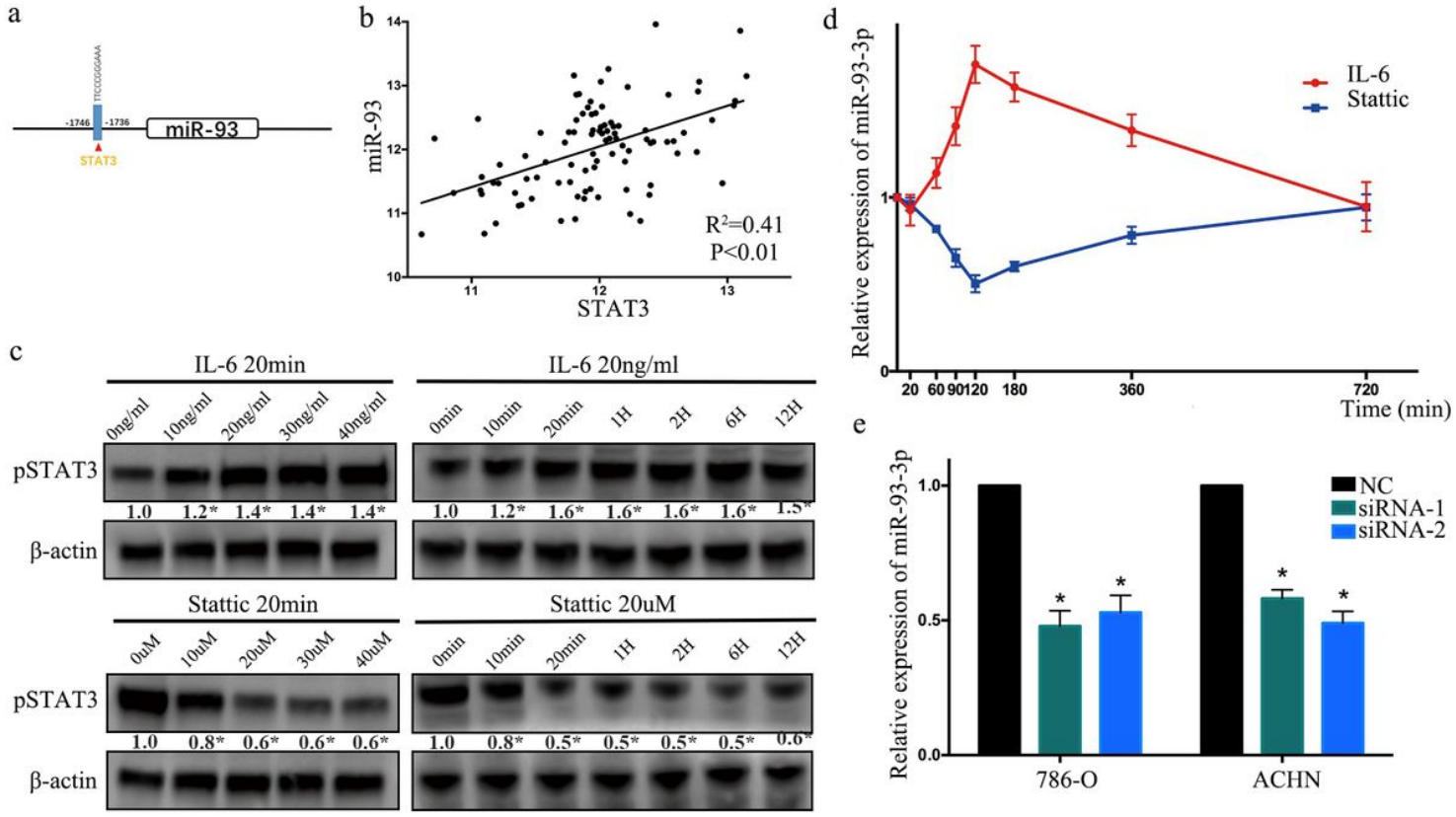

Figure 3

STAT3 up-regulated the expression miR-93. a, Schematic of miR-93 promoter. The predicted STAT3 binding sites were located at -1736 to -1746. b, The correlation between the expression of STAT3 and miR-93. c, The optimum concentration and effective time range of the activator and inhibitor of STAT3. IL6 and Stattic launched their effect after added in 20 mins. d, The time-miR93 curve after 786-O cells treated under 20ng/ml and 20μM Stattic. e, Relative expression of miR-93-3p in siRNA treated cells.

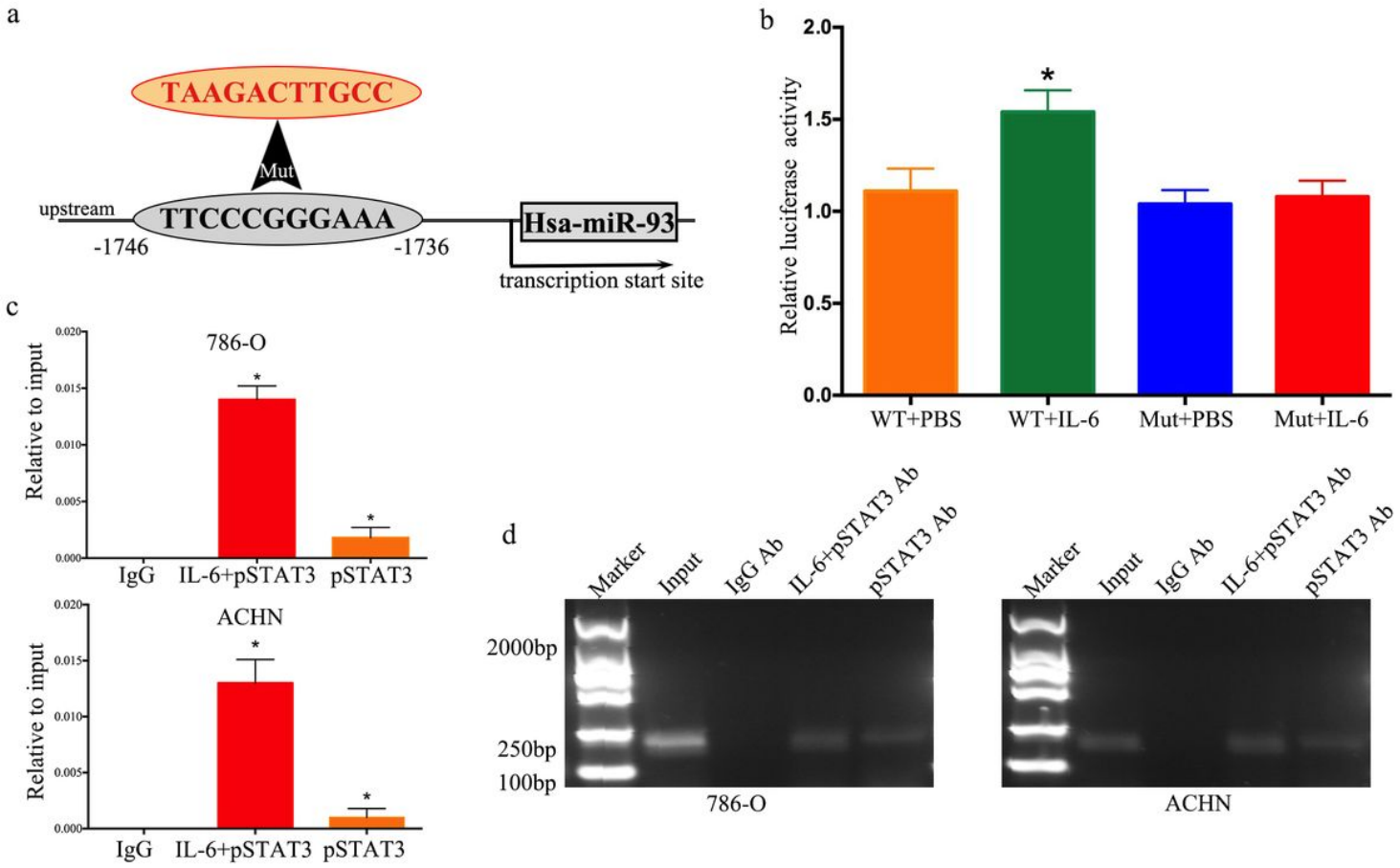

Figure 4

STAT3, as a transcripiton factor, bound with the promoter region of miR-93. a, miR-93 promoter region was cloned into a pmirGLO luciferase reporter plasmid. For the mutant type, 10 nucleotides at the predicted binding site were altered simultaneously. b, Luciferase assay results showed that activation of STAT3 significantly increased the luciferase activity in cells transfected with luciferase reporter plasmid containing the wild-type miR-93 promoter. c, qRT-PCR was also performed to measure the enrichment of predicted binding fragments. d, ChIP assay results showed that STAT3 physically bound with the miR-93 promoter. Lane 1, input chromatin prior to IP. Lane 2, IP with the non-specific antibody, IgG. Lane 3, IP with pSTAT3 antibody when IL6-stimulating. Lane 4, IP with just pSTAT3.

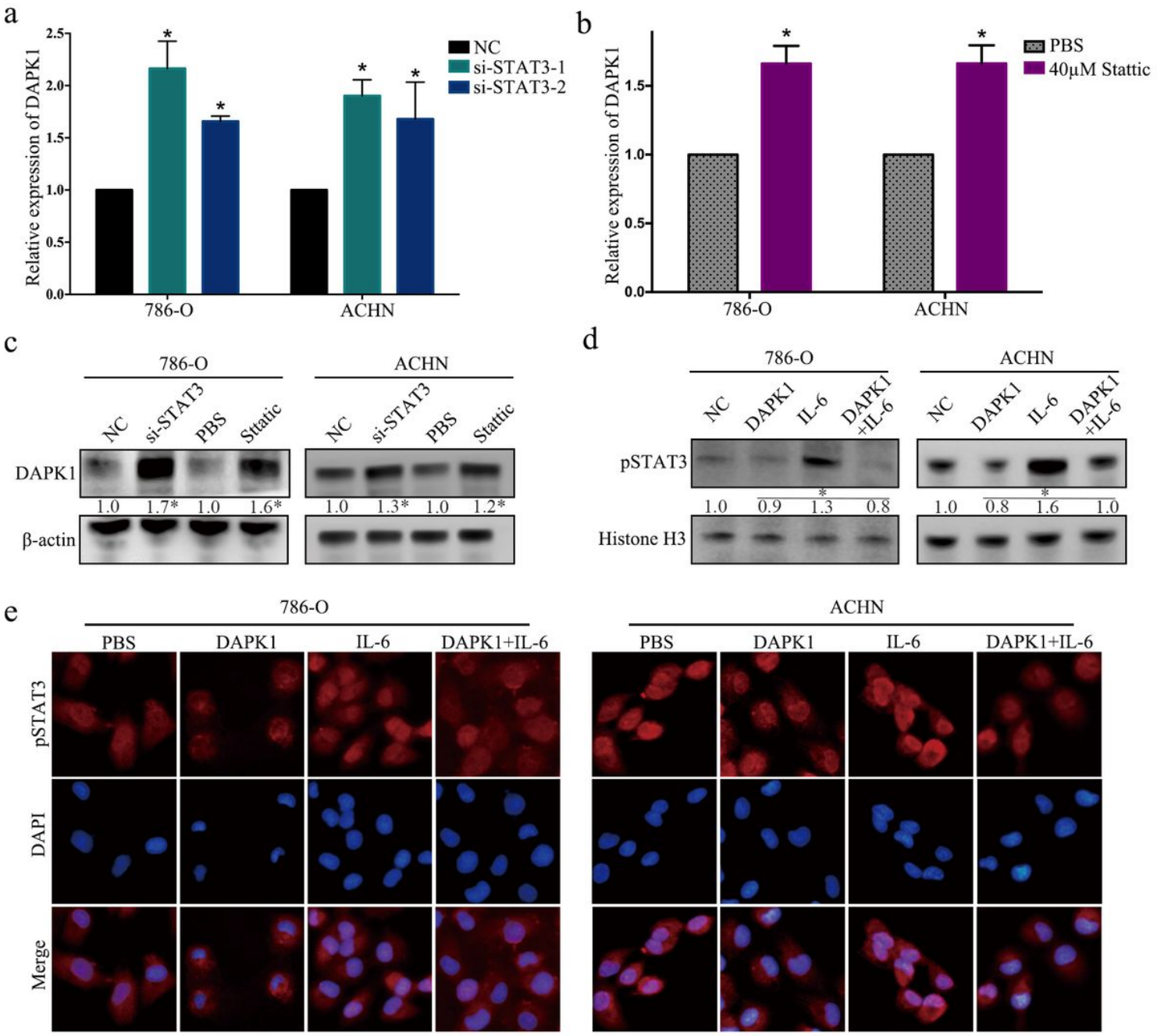

Figure 5

STAT3 inhibited the mRNA and protein level of DAPK1, and DAPK1 deactivated STAT3. a, Relative expression of DAPK1 measured in qRT-PCR after two cell lines treated by siRNA. b, Relative expression of DAPK1 measured in qRT-PCR when STAT3 inactivation. c, The protein expression of DAPK1 among different groups with STAT3 knockdown and inactivation. d, pSTAT3 in nuclear proteins extracted were measured by western blot analysis. e, Immunofluorescence assay showed that DAPK1 attenuated pSTAT3 entry into nuclear.

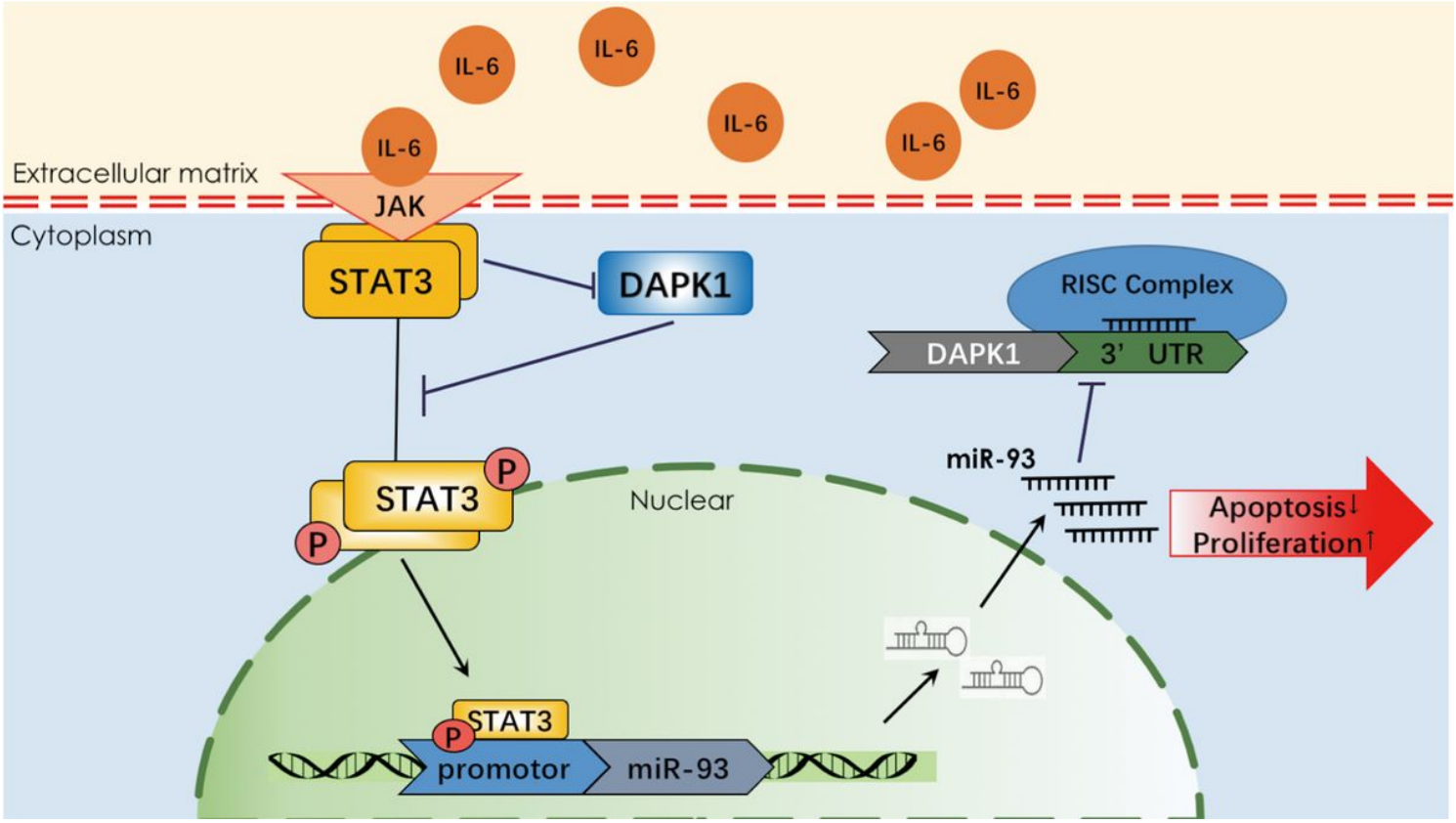

Figure 6

STAT3 regulates miR93-mediated apoptosis through inhibiting DAPK1 in Renal cell carcinoma. STAT3 promotes miR-93-3p expression by binding to promoter region, then miR-93-3p suppressed DAPK1. What's more, DAPK1 mediates the activation of STAT3 pathway through blocking pSTAT3 translation into the nucleus, and STAT3 decreased the expression of DAPK1.

Supplementary Files

This is a list of supplementary files associated with this preprint. Click to download.

- SupplementalFigure.jpg
- SupplementalFigure.jpg